Hyperbranched Poly(ferrocenylphenylenes): Synthesis, Characterization, Redox Activity, Metal Complexation, Pyrolytic Ceramization, and Soft Ferromagnetism

Jianbing Shi,[†] Bin Tong,[†] Zhen Li,[§] Jinbo Shen,[†] Wei Zhao,[†] Huanhuan Fu,[†] Junge Zhi,[‡] Yuping Dong,*[,†] Matthias Häussler,[§] Jacky W. Y. Lam,[§] and Ben Zhong Tang*[,§]

College of Materials Science & Engineering, College of Science, Beijing Institute of Technology, Beijing 100081, China, and Department of Chemistry, The Hong Kong University of Science & Technology, Clear Water Bay, Kowloon, Hong Kong, China

Received May 4, 2007; Revised Manuscript Received August 19, 2007

ABSTRACT: Hyperbranched poly(ferrocenylphenylenes) (*hb*-PFPs) with high molecular weights were synthesized by the copolycyclotrimerizations of (*E*,*E*)-1,1′-bis[2-(4-ethynylphenyl)vinyl]ferrocene (**1**) with (*E*)-1-[2-(4-ethynylphenyl)vinyl]ferrocene (**2**) catalyzed by $TaCl_5-Ph_4Sn$ at room temperature in high yields (up to 97%). Effects of reaction conditions, such as monomer and catalyst concentrations, reaction time and molar feed ratio ($r_{1/2}$), on the copolycyclotrimerization were investigated. Solubility of the copolymer is decreased with an increase in its content of diyne component (N_1/N_2). The *hb*-PFPs were characterized by IR, NMR, UV, CV and TGA analyses. The copolymers are redox active, whose oxidation potentials are decreased with an increase in N_1/N_2. They are thermally stable, losing ∼5% of weights when heated to 384−400 °C and retaining ∼70% of weights when pyrolyzed at 1200 °C. The complexation with cobalt carbonyl further metallizes the *hb*-PFPs and the pyrolytic ceramization of the cobalt−polymer complexes yields soft ferromagnetic ceramics with high magnetizability (M_s up to ∼126 emu/g) and low coercivity (H_c down to ∼0.068 kOe).

Introduction

Organometallic polymers are emerging as a new class of advanced functional materials. The impetus for developing these materials is based on the premise that the metal-containing polymers may exhibit properties difficult to achieve, or ones that are completely inaccessible, by use of their pure organic congeners. Indeed, the attributes from the organic and metallic components of the polymers have led to the generation of new materials with liquid crystallinity, magnetic susceptibility, photonic responses, and catalytic activity[1] and have enabled the polymers to find an array of unique applications, such as the redox-control of sizes and shapes of macroscopic objects and the selective binding and sensing of molecular hazards, metallic ions, and bioactive species.[2]

Ferrocene is an archetypical organometallic compound. Because of its special electrical and chemical properties, much effort has been devoted to its incorporation into polymers.[3,4] Manners and co-workers have synthesized linear poly(ferrocenylsilanes) by thermally induced, transition metal-catalyzed, and anionic and photolytic ring-opening polymerizations.[5] The polymers show novel chemical and physical properties and can function as catalyst seeds for the growth of carbon nanotubes.[6] Abd-El-Aziz et al. have worked on the synthesis and characterization of linear and star polymers with ferrocenyl units in the main chains or side chains.[7]

Our research groups have prepared hyperbranched poly(ferrocenylsilyne)s by desalt polycoupling of dilithiated ferrocene with trichlorosilanes.[8] Upon sintering at high temperatures under nitrogen or argon, the organoiron polymers are converted into ceramics containing iron nanoclusters. The hyperbranched polymers ceramized in higher yields than their linear congeners. When magnetized at room temperature by an external magnetic field, the ceramics exhibited high saturation magnetization (M_s) and near-zero remanence (M_r) and coercivity (H_c). In other words, the ceramics are excellent magnetic materials with low hysteresis losses. The hyperbranched polymers are, however, weakly electronically conjugated due to the existence of sp^3-hybridized silicon atoms in their branches.

We are interested in the creation of organometallic polymers with extended electronic conjugations. We have recently developed new approaches to hyperbranched conjugative polymers using acetylenes with multiple triple bonds as A_n-type monomers[9] and succeeded in the preparations of hyperbranched polyphenylenes through transition polycyclotrimerizations of aromatic diynes.[10] The polymers show high thermal stability, emit efficiently upon photoexcitation, and display strong optical nonlinearity.[11] In our previous work, we studied the copolycyclotrimerizations of (*E*)-1-[2-(4-ethynylphenyl)vinyl]-ferrocene (**2**; a ferrocenyl monoyne) with 1,8-nonadiyne (an aliphatic diyne)[12] or 4,4′-diethynylbiphenyl (an aromatic diyne).[13] The copolycyclotrimerization reactions proceeded smoothly, giving ferrocene-containing hyperbranched copolymers in good yields. However, governed by the chemical reactivity of the monoyne, the ferrocenyl groups are mainly located in the peripheries of the hyperbranched polymers.

In this work, we extended our effort in the area, with the aim of synthesizing new hyperbranched conjugated organometallic polymers with the ferrocenyl groups distributed in the whole polymer structures, that is, not only on the shells and but also in the cores. To accomplish this goal, we designed and prepared a new ferrocene-containing diyne monomer of (*E*,*E*)-1,1′-bis[2-(4-ethynylphenyl)vinyl]-ferrocene (**1**). Its copolymer-

* To whom correspondence should be addressed. (Y.P.D.) Fax: +86-10-6894-8982. E-mail: chdongyp@bit.edu.cn. (B.Z.T.) Fax: +852-2358-1594. E-mail: tangbenz@ust.hk.

† College of Materials Science & Engineering, Beijing Institute of Technology.

‡ College of Science, Beijing Institute of Technology.

§ The Hong Kong University of Science & Technology.

10.1021/ma071019q CCC: $37.00
Published on Web 10/12/2007

Scheme 1

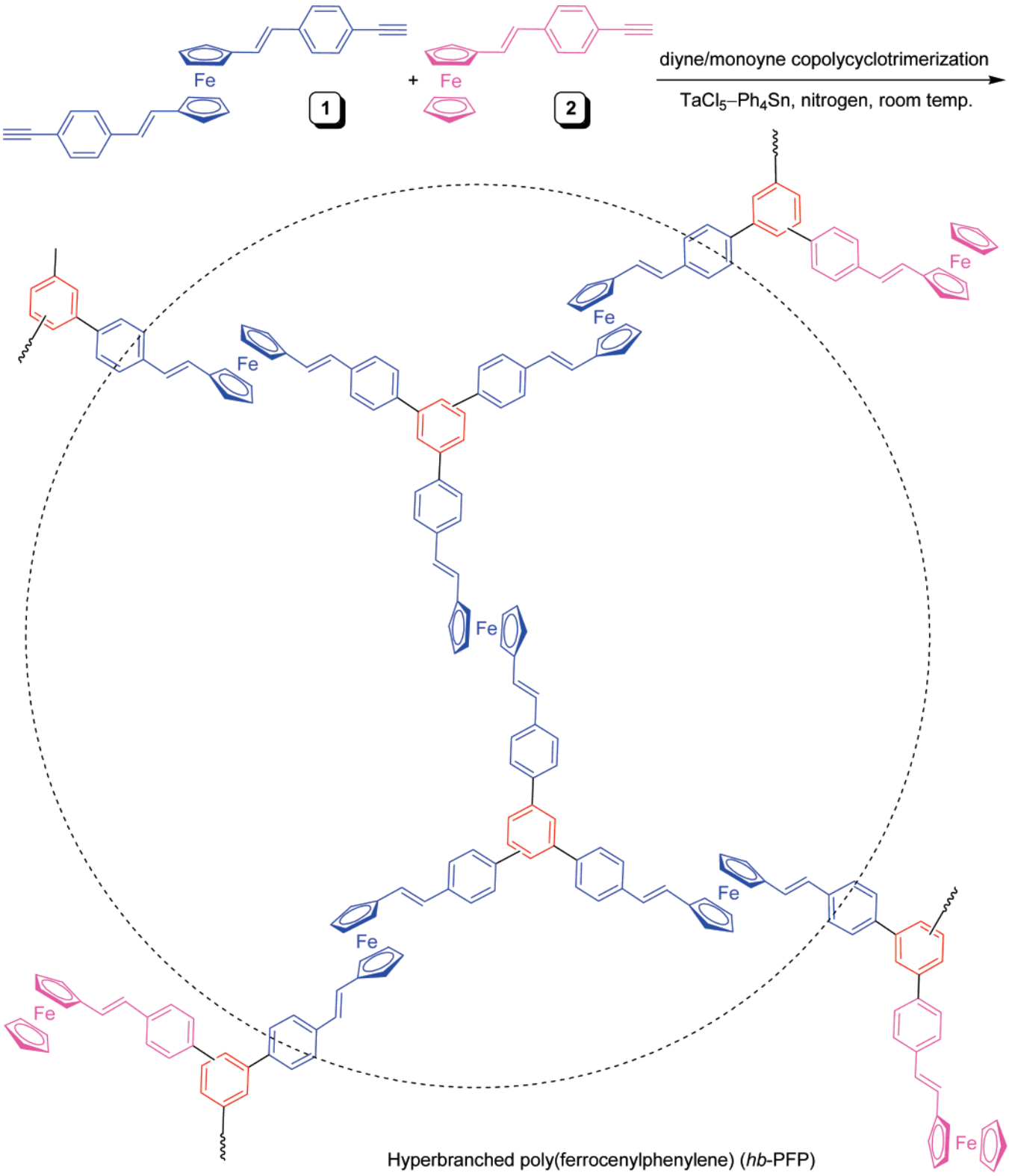

izations with monoyne **2** catalyzed by a mixture of $TaCl_5$ and Ph_4Sn at room-temperature gave hyperbranched poly(ferrocenylphenylenes) (*hb*-PFPs), the expected products of fully "ferrocenated" polymers, in high yields (Scheme 1). The *hb*-PFPs are soluble, stable, and redox active. Their further metallization by cobalt carbonyl[14] afforded cobalt−polymer complexes that served as precursors to soft ferromagnetic ceramics.

Results and Discussion

Synthesis. The ferrocene-containing diyne monomer (**1**) was prepared by the published procedures[15] with modifications, according to the synthetic route shown in Scheme 2. An isomeric mixture of 1,1′-bis[2-(4-bromophenyl)vinyl]ferrocenes with (*E*/*E*)-, (*E*/*Z*)-, and (*Z*/*Z*)-conformations was prepared by the Wittig reaction of Wittig reagent **4** and 1,1′-ferrocenedicarboxyaldehyde (**5**). Recrystallization from hexanes separated (*E*/*E*)-isomer **6**

Scheme 2

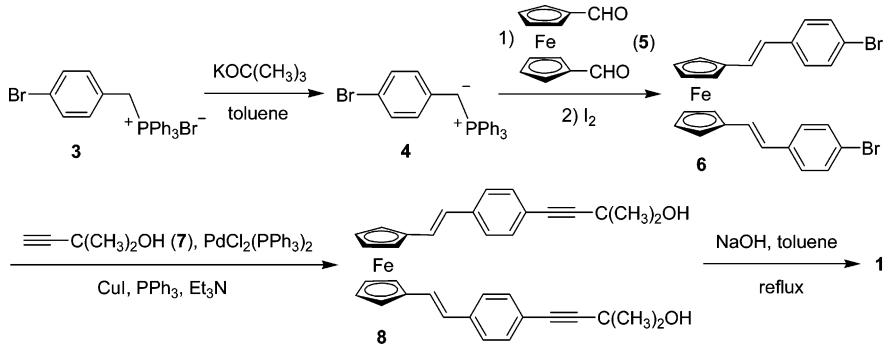

Scheme 3

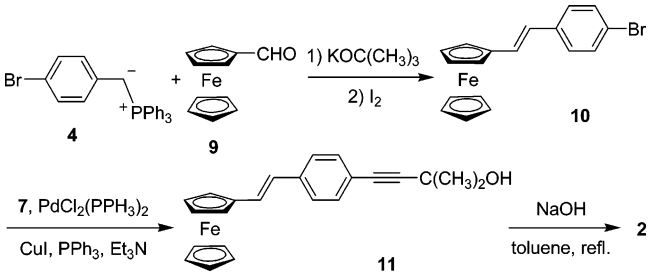

from the mixture, and the (*E*/*Z*)- and (*Z*/*Z*)-isomers left in the solution was transformed to **6** quantitatively by iodine-catalyzed isomerization. Palladium-catalyzed coupling of **6** with **7** followed by base-catalyzed deprotection afforded the desired diyne monomer (**1**). Monoyne **2** was prepared by the similar synthetic procedures, using ferrocenecarboxyaldehyde **9**, instead of **5**, as a reactant (Scheme 3). Both the diyne and monoyne monomers were characterized spectroscopically, from which satisfactory analysis data were obtained (see Experimental Section for details).

Many complexes of late transition metals such as cobalt and palladium are good catalysts for alkyne cyclotrimerizations. In our previous study, we have obtained hyperbranched polyphenylenes from the copolymerizations of 4,4′-diethynylbiphenyl with **2** catalyzed by $CpCo(CO)_2-h\nu$.[13] We attempted to use the same catalyst to initiate the copolymerizations of **1** with **2** in this study, but disappointingly, no polymeric products could be isolated, no matter how we had changed the reaction conditions (feed ratio, catalyst concentration, reaction temperature, etc.). The diyne and monoyne may have been converted to low molecular weight oligomers that are soluble in the solvents used in the polymer purification process, hence the failure in the product isolation.

We then checked whether $TaCl_5-Ph_4Sn$, an effective catalyst for polycyclotrimerizations of aliphatic and aromatic diynes,[9,16] could initiate the copolymerizations of **1** with **2**. When a mixture of **1** and **2** with a feed ratio ($r_{1/2}$) of 1 was stirred in the presence of the tantalum catalyst at room temperature, an *hb*-PFP with an M_w value of 3100 was obtained in ∼91% yield in 30 min (Table 1, no. 1). Increasing the monomer and catalyst concentrations from 25 and 3.75 mM to 50 and 7.5 mM, respectively, results in increases in both polymer yield and molecular weight (Table 1, no. 2).

The M_w values seem rather small, which may, however, not be the real values of the *hb*-PFPs but a technical problem associated with the GPC system calibrated by the linear polystyrene standards, which commonly underestimates molecular weights of hyperbranched polymers.[17] Deffieux and coworkers, for example, used a "normal" GPC system equipped with a RI detector (GPC/RI; linear polystyrene calibration) and an "advanced" GPC system equipped with RI and laser light scattering dual detectors (GPC/RI/LLS) to measure the molecular weights of hyperbranched polystyrenes and found that the M_n values estimated by the GPC/RI system were normally ∼7-fold, sometimes ∼30-fold, lower than those determined by the GPC/RI/LLS system.[17b] To get the real M_w values of the *hb*-PFPs, we measured their molecular weights by a GPC system equipped with RI and multiangle laser light scattering detectors (GPC/RI/MALLS). Similar to what observed in other hyperbranched polymer systems, the absolute M_w values of our *hb*-PFPs are much higher than their polystyrene-calibrated relative values (Table 1, nos. 1 and 2). Clearly, the copolycyclotrimerizations of diyne **1** and monoyne **2** can produce soluble *hb*-PFPs with high molecular weights in excellent yields.

We systematically investigated the behaviors of the diyne/monoyne copolycyclotrimerizations, in an effort to optimize the reaction conditions. The copolymerization carried out at $[C\equiv C]_t = 50$ mM and [cat.] = 7.5 mM gives an *hb*-PFP with an M_w value of 17800 in ∼96% yield. Increasing the monomer and/or catalyst concentrations does not help much or even has a reverse effect on the polymer yield and molecular weight (Table 1, no. 2 vs nos. 3−5). The monomer and catalyst concentrations are thus fixed at 50 and 7.5 mM, respectively, in our further investigations.

The time course of the copolymerization reaction was followed. The copolymerization conducted at the "optimal" monomer and catalyst concentrations affords a copolymer with an M_w value of 19800 in ∼77% yield in 10 min (Table 1, no. 6). Prolonging the polymerization time to 30 min results in an increase in the polymer yield (∼96%). The yield is decreased to ∼91% when the reaction is further lengthened to 120 min, possibly due to the formation of high molecular weight species that is insoluble and hence filtered out in product purification process.

The polycyclotrimerizations were then conducted at different feed ratios. At $r_{1/2} = 0.5$, an *hb*-PFP with an M_w value of 8400 is produced in ∼87% yield (Table 1, no. 8). Increasing $r_{1/2}$ to 1 boosts the polymer yield and molecular weight, which is understandable, because diyne **1** is the real contributing monomer, whereas monoyne **2** does not only serve as a comonomer but also can work as a terminator. Further increasing the $r_{1/2}$ value to 2 results in the formation of an *hb*-PFP whose GPC curve is bimodal (Figure 1), with the molecular weight associated with the first peak being as high as 683700. The copolymers produced by the reactions at even higher $r_{1/2}$ values are only partially soluble, due to the involvement of cross-linking reactions in these systems.

Characterization. The *hb*-PFPs were characterized by spectroscopic techniques. All the copolymers gave satisfactory analysis data corresponding to their expected molecular struc-

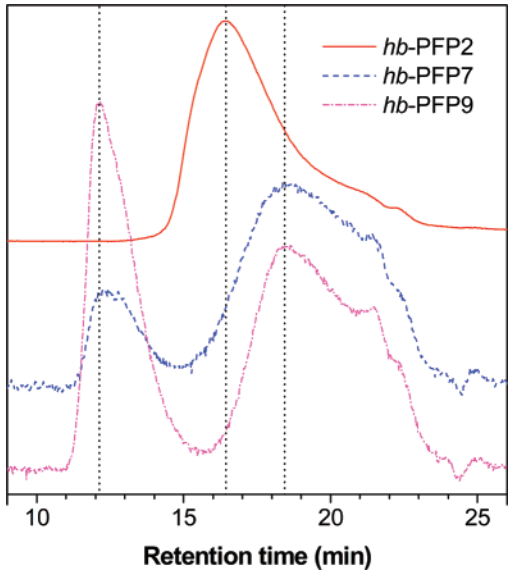

Figure 1. Examples of MALLS-GPC chromatograms of *hb*-PFPs (samples taken from Table 1, nos. 2, 7 and 9).

Table 1. Copolycyclotrimerizations of Diyne 1 with Monoyne 2[a]

						UV[d]		MALLS[e]		
no.	$r_{1/2}$[b]	[C≡C]$_t$[c] (mM)	[cat.] (mM)	time (min)	yield (%)	M_w	PDI	M_w	PDI	S[f]
1	1	25	3.75	30	90.8	3100	2.6	13 380	2.80	√
2	1	50	7.5	30	95.9	3200	2.6	17 800	3.43	√
3	1	100	10	30	65.2	2200	2.1	22 100	2.88	√
4	1	100	15	30	97.1	2600	2.3	15 500	3.03	√
5	1	100	20	30	88.3	2800	2.4	20 700	1.14	√
6	1	50	7.5	10	77.3	4000	2.9	19 800	2.82	√
2	1	50	7.5	30	95.9	3200	2.6	17 800	3.43	√
7	1	50	7.5	120	91.2	2900	2.4	5800[g]	1.85	√
8	0.5	50	7.5	30	86.6	2300	2.1	8400	2.44	√
2	1	50	7.5	30	95.9	3200	2.6	17 800	3.43	√
9	2	50	7.5	30	95.3	2100	2.0	6000[g]	1.85	√
10	6	50	7.5	30	95.0	2100	1.9	3100	1.42	Δ
11	10	50	7.5	30	90.6	2200	2.0	4700	1.50	Δ

[a] Carried out in toluene under nitrogen at room temperature using $TaCl_5$-Ph_4Sn as catalyst ([$TaCl_5$] = [Ph_4Sn]). [b] Molar feed ratio of **1** to **2**. [c] Total concentration of triple bonds. [d] Estimated by a GPC system equipped with a UV detector on the basis of a polystyrene calibration. M_w = weight-average molecular weight. PDI = polydispersity index (M_w/M_n). [e] Estimated by a GPC system equipped with a multiangle laser light scattering (MALLS) detector. [f] Solubility tested in common organic solvents such as THF, dichloromethane (DCM), chloroform, toluene, DMF, and DMSO. Symbol: √ = completely soluble, Δ = partially soluble. [g] Value for the second peak (cf., Figure 1).

tures. An example of IR spectrum of an *hb*-PFP is shown in Figure 2; those of its monomers are also given in the same figure for comparison. The ≡C−H stretching and bending bands of diyne **1** are observed at 3276 and 617 cm−1, respectively, while those of monoyne **2** are found at 3264 and 625 cm−1. The C≡C stretching bands are observed at ∼2100 cm^{-1}. These bands are absent in the spectrum of the *hb*-PFP, indicating that the triple bonds have all been consumed by the polycyclotrimerization reaction.

Figure 3 shows the ^{1}H NMR spectra of an *hb*-PFP and its monomers. The signals of the copolymer can be readily assigned by comparison with those of its monomers. The resonance peaks of the *hb*-PFP are broader than those of its monomers due to its rigid and irregular molecular structure, comprising of a random mixture of 1,2,4- and 1,3,5-trisubstituted benzene isomers ($V_{1,2,4}$ and $V_{1,3,5}$; Scheme 4). The *hb*-PFP shows no

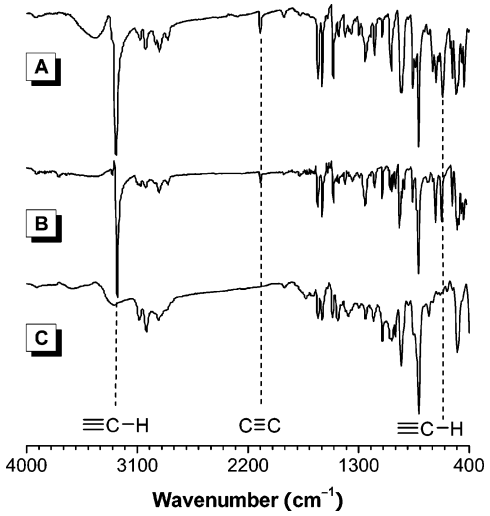

Figure 2. IR spectra of (A) diyne **1**, (B) monoyne **2** and (C) their copolymer *hb*-PFP9 (sample taken from Table 1, no. 9).

resonance peaks of acetylene protons at $\delta \sim 3.1$, confirming that **1** and **2** have undergone alkyne polycyclotrimerization and revealing that **2** has also served as an end-capping agent to consume the acetylenic triple bonds on the periphery or shell of the copolymer (Scheme 5). The new peaks in the region of $\delta \sim 7.5-7.8$ may be associated with the resonances of the protons of the 1,2,4- and 1,3,5-trisubtituted benzene rings newly formed in the copolycyclotrimerization reaction.

The new peaks in the chemical shift region of $\delta \sim 6-6.5$ suggest that the *hb*-PFP contains butadiene groups. According to our previously proposed polycyclotrimerization mechanism, the active Ta species oxidatively adds to an acetylene triple bond (I) to form a tantallacyclopropene species (II; Scheme 4).[11b] Insertion of another triple bond to II may afford three tantallacyclopentadiene regioisomers (III), among which, the likelihood to form IIIc is the lowest because of the involved steric effect. Addition of a third triple bond to IIIa can yield two tantallacycloheptatriene species (IVaa) and two Diels−Alder adducts of tantallanorbornadienes (IVab), each possessing different steric properties but all giving same product of $V_{1,2,4}$. On the other hand, addition of a triple bond to IIIb furnishes a tantallacycloheptatriene (IVba) and a tantallanorbornadiene (IVbb), whose reductive elimination yields $V_{1,3,5}$. When the polymerization is stopped by the addition of methanol into the reaction mixture, premature termination of III leads to the formation of butadiene species VIII (Scheme 5), which may well be responsible to the observed ^{1}H NMR peaks in the olefin resonance region (Figure 3C).

To gain more structural insights, the areas of the proton resonance peaks of the *hb*-PFPs are integrated and analyzed. As can be seen from Figure 3C, the resonance peak of the copolymer at δ 4.15 is solely associated with its monoyne component, while those at δ 4.29 and 4.50 are related to both the monoyne and diyne components. The ratio of the numbers of diyne unit (N_1) to monoyne unit (N_2) of the *hb*-PFP can thus be calculated by eq 1:

$$\frac{N_1}{N_2} = \frac{(A_{4.50} + A_{4.29} - 4A_{4.15}/5)/8}{A_{4.15}/5} \quad (1)$$

where $A_{4.50}$, $A_{4.29}$, and $A_{4.15}$ are the integrated areas of proton resonance peaks at δ 4.50, 4.29 and 4.15, respectively. The calculated compositions (N_1/N_2) of the copolymers are close to

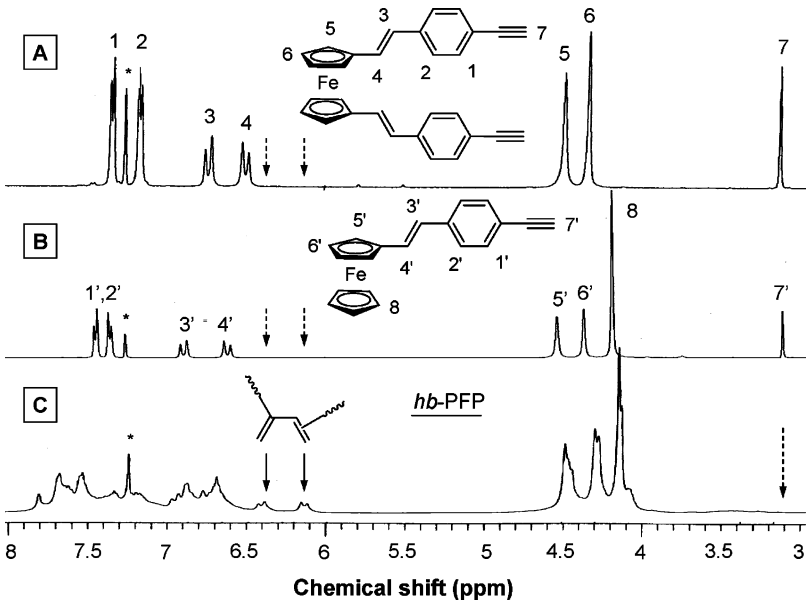

Figure 3. ^{1}H NMR spectra of (A) diyne **1**, (B) monoyne **2** and (C) their copolymer *hb*-PFP8 (sample taken from Table 1, no. 8) in chloroform-*d*. The solvent peaks are marked with asterisks.

Scheme 4

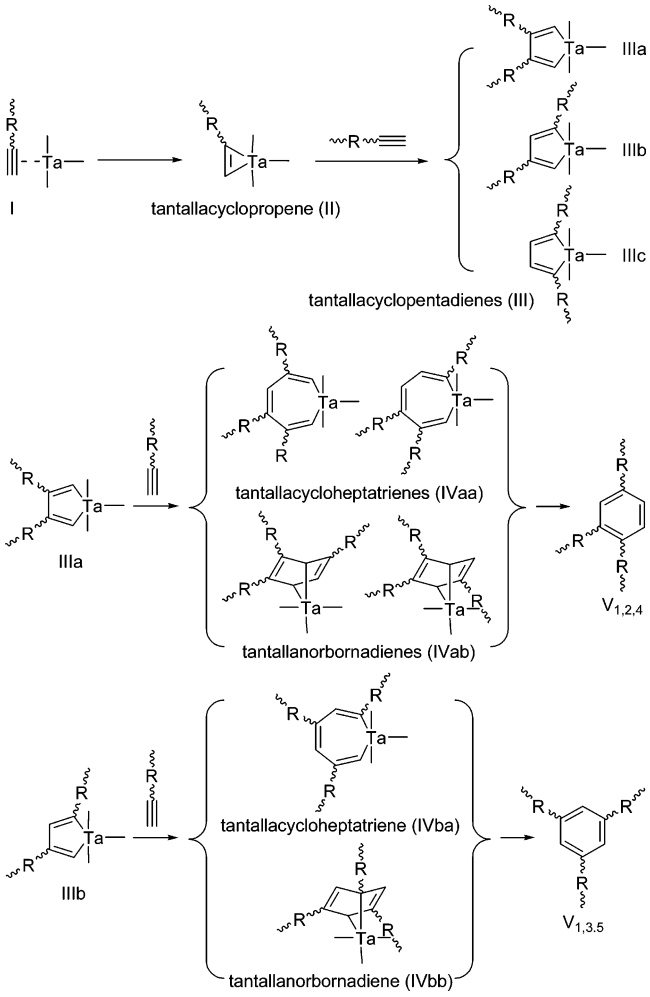

Scheme 5

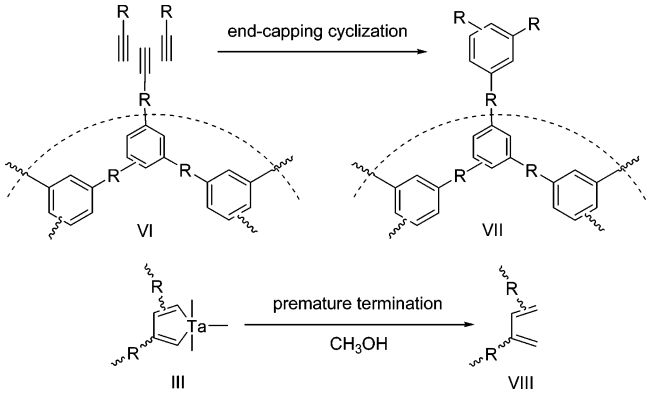

Table 2. Compositions of *hb*-PFPs

no.[a]	$r_{1/2}$	N_1/N_2
8	0.5	0.7
9	2	2.4
10	6	5.5
11	10	8.7

[a] Corresponding to the numbers in Table 1.

the feed ratios ($r_{1/2}$) of the comonomers (Table 2), indicating that the two monomers have similar reactivity or polymerizability. In other words, the copolymer compositions can be readily tuned by changing their monomer fee ratios.

Properties. Figure 4 shows the absorption spectra of THF solutions of *hb*-PFPs and their diyne and monoyne monomers. The absorption peak of monoyne **2** locates at ~325 nm, while diyne **1** exhibits a peak at ~309 nm with a shoulder at ~343 nm. The copolymers absorb in the redder spectral region, with an absorption peak at ~328 nm. The shoulders originating from the diyne components of the *hb*-PFPs are now buried under their main peaks. The shoulder red shifts with an increase in the diyne content, suggesting that the copolymer with a higher content of diyne units possesses a more extended electronic conjugation.

The *hb*-PFPs are redox active and show cyclic voltammograms associated with ferrocene/ferricinium redox couples (Figure 5). No high degree of Fe−Fe interaction is observed in the redox processes of the copolymers, suggestive of a lack of electronic communication between the metallic species.[18,19] It is well-known that for a fully reversible redox system, $i_p^a/i_p^c = 1$ and $\Delta E_p = 57/n$ (mV), where n is the number of electron equivalents transferred during the redox process. This is not the case for the *hb*-PFPs or their redox processes are not fully reversible, as can be understood from the data given in Table 3. The oxidation potential (E_p^a) of the copolymer is linearly

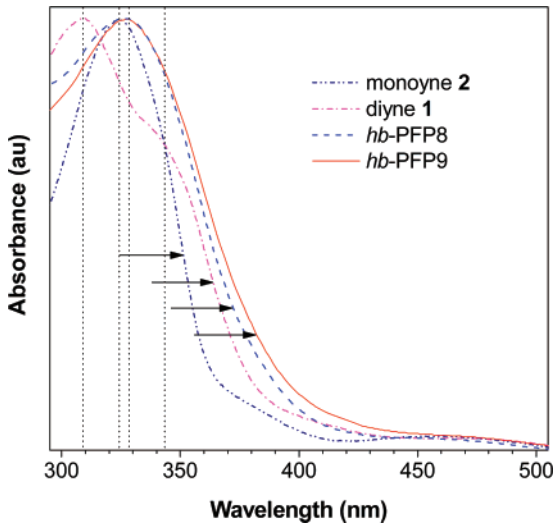

Figure 4. Normalized absorption spectra of dilute THF solutions (5−10 μg/mL) of monomers **1** and **2** and their copolymers *hb*-PFP8 and *hb*-PFP9 (samples taken from Table 1, nos. 8 and 9).

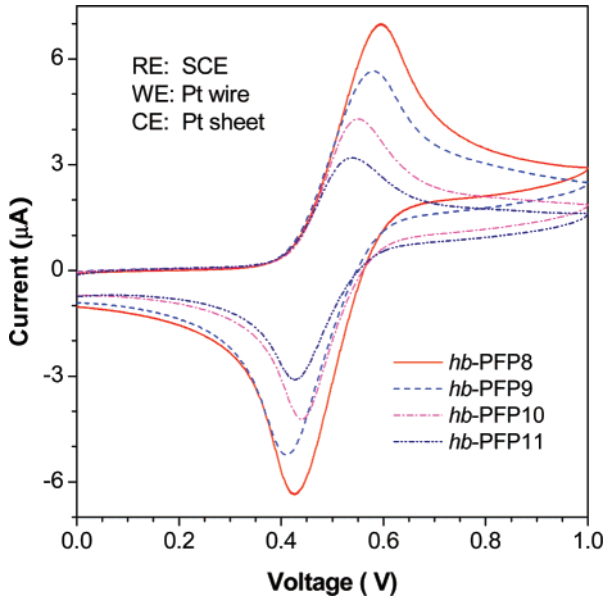

Figure 5. Cyclic voltammograms of *hb*-PFP8−11 (sample taken from Table 1, nos. 8−11) measured at 25 °C in THF containing 0.1 M of *n*-Bu_4NPF_6 at a scan rate of 100 mV/s.

Table 3. Electrochemical and Thermal Properties of *hb*-PFPs[a]

no.[b]	i_p^a (μA)	i_p^c (μA)	E_p^a (V)	E_p^c (V)	ΔE (V)	T_d (°C)	W_r (%)
8	6.315	−7.378	0.595	0.426	0.169	384	72
9	5.253	−5.979	0.581	0.409	0.172	428	70
10	4.106	−4.897	0.550	0.440	0.110	436	70
11	2.962	−3.530	0.539	0.428	0.111	451	69

[a] Abbreviations are as follows. i_p^a: anodic peak current. i_p^c: cathodic peak current. E_p^a: anodic peak potential. E_p^c: cathodic peak potential. ΔE: peak potential difference ($E_p^a - E_p^c$). $E_{1/2}$: formal redox potential [($E_p^a + E_p^c$)/2]. T_d: temperature for 5% weight loss. W_r: weight residue after pyrolysis at 1200 °C. [b] Number corresponding to that in Table 1.

decreased with an increase in its diyne content (Figure 6); in other words, the oxidation of the copolymer becomes easier when its diyne content is increased. This is possibly due to the better electronic conjugations in the copolymers with higher diyne contents.[20]

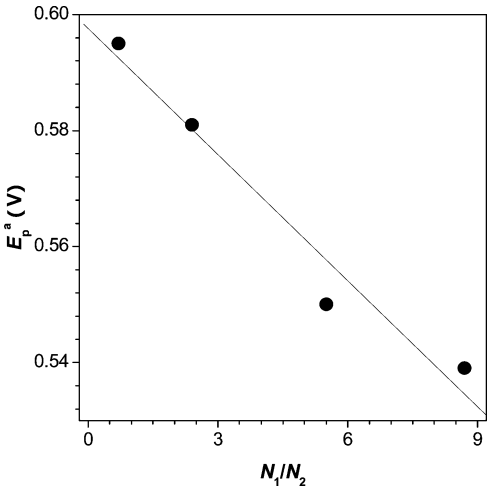

Figure 6. Variation of oxidation potential (E_p^a) of *hb*-PFP with its molar composition (N_1/N_2).

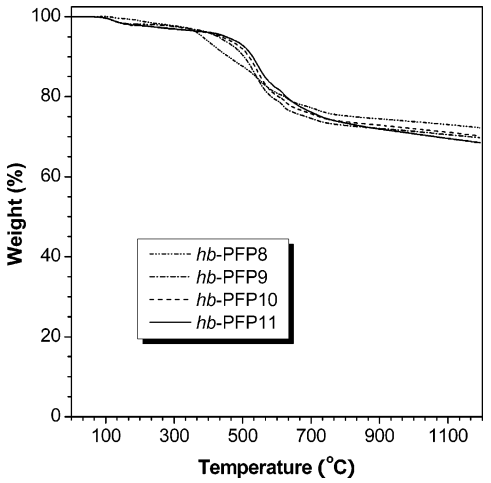

Figure 7. TGA thermograms of *hb*-PFP8−11 (samples taken from Table 1, nos. 8−11) recorded under nitrogen at a heating ratio of 10 °C/min.

Scheme 6

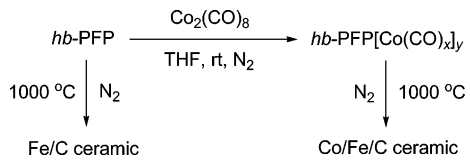

Thermal stability of the *hb*-PFPs was evaluated by thermogravimetric analysis (TGA) under nitrogen. As shown in Figure 7, all the copolymers are thermally very stable, losing merely 5% of their weights when heated to temperatures up to ~450 °C. The thermal stability of the *hb*-PFP is increased with an increase in its content of diyne component (Table 3). The diyne unit contains more benzene rings and vinyl groups. The former is thermally robust, while the latter can be thermally polymerized to form a cross-linked network structure, both contributing to the enhanced thermal stability of the copolymers. The weight residues of the *hb*-PFPs after pyrolysis at 1200 °C are as high as ~70%, revealing that the copolymers are promising precursors to ceramic materials. The pyrolysis products can be attracted to a bar magnet, due to the formation of iron nanoparticles in the ceramization process.

The copolymers contain π electron-rich benzene and ethylene units as well as butadiene groups (cf., Scheme 5), all of which

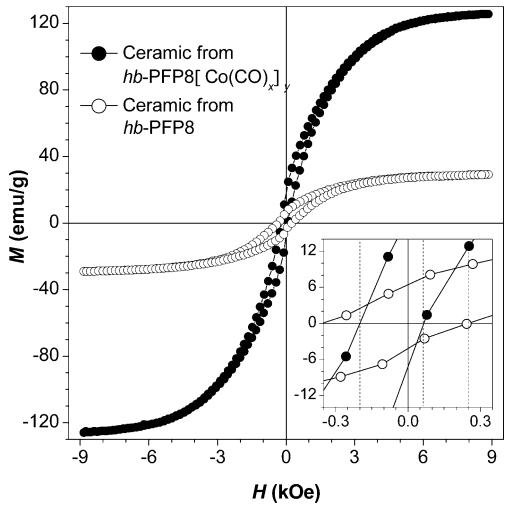

Figure 8. Plots of magnetization (***M***) vs applied magnetic field (***H***) at 300 K for ceramics fabricated from *hb*-PFP8 and *hb*-PFP8[$Co(CO)_x]_y$. Inset: enlarged portions of the ***M*-*H*** plots in the low magnetic field region.

Table 4. Pyrolyses of *hb*-PFPs and Their Cobalt Complexes and Magnetizations of Their Ceramization Products

sample	ceramic yield (%)	M_s (emu/g)
hb-PFP8	68.8	29
hb-PFP8[$Co(CO)_x]_y$	52.9	126
hb-PFP9	69.9	24
hb-PFP9[$Co(CO)_x]_y$	54.7	114
hb-PFP10	71.8	23
hb-PFP10[$Co(CO)_x]_y$	54.8	114
hb-PFP11	70.9	23
hb-PFP11[$Co(CO)_x]_y$	57.0	111

can form complexes with cobalt carbonyls.[21] Indeed, when an *hb*-PFP is mixed with $Co_2(CO)_8$ in THF, the solution instantly changes from red to brown in color, accompanying with gas evolution. This clearly verifies the occurrence of the cobalt complexation reaction (Scheme 6). The solution remains homogeneous throughout the whole process of complexation reaction. However, the isolated product is insoluble, possibly due to the formation of supramolecular aggregates during the product purification processes.

We have previously found that hyperbranched organometallic polymers, in comparison to their linear counterparts, are better precursors to magnetic ceramics in terms of ceramization yield and magnetic susceptibility because the three-dimensional cages of hyperbranched polymers enable better retention of pyrolyzed species and steadier growth of magnetic crystallites.[8,14b,22] Pyrolyzing the *hb*-PFPs and their cobalt complexes in a tube furnace at 1000 °C for 1 h under nitrogen give ceramic products in ~53−72% yields (Table 4). The ceramization yields of the cobalt−polymer complexes are always lower than those of their parent polymers, which is easy to understand, because the volatile CO species of the complexes are lost during the heating process.

All the ceramics are magnetizable. Typical examples of the magnetization curves of the ceramics are shown in Figure 8. Under an externally applied magnetic field, the iron-nanoparticle-containing ceramic prepared from *hb*-PFP8 is magnetized and then quickly saturated at 29 emu/g. The magnetization rate of the ceramic prepared from its cobalt complex, i.e., *hb*-PFP8-[$Co(CO)_x]_y$, is much faster. Evidently, the cobalt nanoclusters in the ceramic have helped to dramatically enhance its magnetic susceptibility. The outstanding magnetizability of the ceramic is evidenced by its impressively high M_s value (126 emu/g), taking into account that the M_s value of maghemite (γ-Fe_2O_3) is 74 emu/g.[23] Manners' research group has prepared magnetic ceramics from the complexes of a linear poly(ferrocenylsilane) and $Co_2(CO)_8$ and found that their M_s values are in the range of ~20−35 emu/g.[24] The M_s value of our ceramic is 3.6−6.3 times higher, once again proving that hyperbranched polymer complexes are better precursors to magnetic ceramics than their linear congeners.

Similar to *hb*-PFP8[$Co(CO)_x]_y$, other cobalt−polymer complexes are also better precursors than their parent forms and are readily transformed into magnetic ceramics with higher M_s values (Table 4). The stronger magnetizability of these ceramics should be due to their higher metal contents, for it is well-known that M_s is proportional to the number of magnetic species in unit volume. The incorporation of the cobalt nanoparticles into the ceramics does not only boost the magnitude of their magnetization but also change the nature of their magnetism. As can be seen from the enlarged $H-M$ plots in the inset of Figure 8, the hysteresis loop of the ceramic prepared from *hb*-PFP8 is large, with an H_c value up to ~0.35 kOe, indicative of a hard magnetism. With the embedment of the cobalt nanoparticles in the ceramic, the H_c value drops to as low as ~0.07 kOe, changing the ceramic to a soft ferromagnetic material.

Conclusions

We have successfully synthesized hyperbranched polyphenylenes with ferrocene units on the shells and in the cores by the tantalum-catalyzed copolycyclotrimerizations of diyne **1** with monoyne **2**. The hyperbranched structures of the *hb*-PFPs are confirmed spectroscopically and chromatographically. The *hb*-PFPs are macroscopically processable, thermally stable, redox active, and cobalt metallizable. The cobalt−polymer complexes are excellent precursors to functional ceramics with high magnetizability and low coercivity.

Experimental Section

Materials. Toluene was distilled over calcium hydride under nitrogen before use. Triethylamine was distilled under normal pressure and kept over potassium hydroxide under nitrogen. Potassium *tert*-butoxide, ferrocenecarboxaldehyde, 1,1′-ferrocenedicarboxaldehyde, triphenylphosphine, copper(I) iodide, dichlorobis(triphenylphosphine)palladium(II), 2-methyl-3-butyn-2-ol, octacarbonyldicobalt, and tetrabutylammonium hexafluorophophate were purchased from Alfa Aesar and used as received without further purification. Tetraphenyltin and tantalum(V) chloride were purchased from Aldrich. 4-Bromo-benzyl bromide and 4-bromobenzyltriphenylphosphonium bromide were prepared according to the literature procedures.[15] Other regents and solvents were purchased from Beijing Reagent Co. and used as received.

Instrumentations. The relative molecular weights of the *hb*-PFPs were estimated by a Waters 510 GPC system equipped with RI and UV detectors with its working wavelength set at 254 nm, using monodisperse polystyrenes as calibration standards and THF as eluent at a flow rate of 1.0 mL/min. The absolute molecular weights of the *hb*-PFPs were estimated by another GPC system equipped with RI and MALLS detectors in THF at 38 °C on a Dawn EOS instrument (Wyatt Technology, Ga−As laser, $\lambda = 690$ nm). Two MZ-Gel SD plus GPC columns (10^4 Å and 10^5 Å, MZ Analysentechnik) were used in series. The samples (500 μL) were filtered through PTFE membranes with a pore size of 0.22 μm before being injected into the GPC systems. The scattering signals were collected at 18 different angles from a flowing sample. The refractive index increment (d*n*/d*c*) was determined to be 0.201 in THF at 38 °C on a Optilab DSP (digital signal processing) refractometer (Wyatt Technology; $\lambda = 690$ nm, $c \leq 0.5$ mg/mL).

The IR spectra were measured on a NEXUS-470 FTIR (Nicolet) spectrophotometer using KBr discs. The ^{1}H NMR spectra were recorded on a Bruker ARX-400 spectrometer using deuterated chloroform as solvent and tetramethylsilane (TMS) as internal reference. The UV absorption spectra were measured on a Hitachi U-2800 spectrophotometer. The mass spectra were recorded on a GCT-MS Micromass UK spectrometer operating in electron ionization (EI) mode. The elemental analyses were carried out with an Elementar Vario EL analyzer.

The cyclic voltammetry (CV) analysis were conducted on a CHI660A electrochemical workstation. All the measurements were carried out at room temperature using a conventional three-electrode configuration. The working electrode was a platinum circular electrode with a diameter of 2 mm. The reference was a saturated calomel electrode, and the counter electrode was a platinum sheet. The *hb*-PFP solutions (~1 mM) were prepared in distilled THF. NBu_4PF_6 (0.1 M) was used as supporting electrolyte. The CV curves were measured at a scan rate of 0.1 V/s. The TGA analyses were carried out on a Universal V2.6D TA Instruments at a heating rate of 10 °C/min under nitrogen. The magnetization curves were recorded on a Lake Shore 7037/9509-P vibrating sample magnetometer (VSM) at room temperature.

Monomer Preparation. The ferrocene-containing monomers **1** and **2** were prepared according to the synthetic routes shown in Schemes 2 and 3, respectively.

Preparation of 1,1′-Bis[2-(4-bromophenyl)vinyl]ferrocene (6). Into a three-necked, round-bottomed flask under argon in an ice−water bath was added 9.220 g (18 mmol) of 4-bromobenzyltriphenylphosphonium bromide (**4**) in 50 mL of dry toluene. Potassium *tert*-butoxide (3.030 g, 27 mmol) was then added under stirring. The solution color changed to intense orange after 30 min. 1,1′-Ferrocenedicarboxaldehyde (1.452 g, 6 mmol) dissolved in 40 mL of dry toluene was slowly added. The mixture was stirred at room temperature overnight. After solvent evaporation, the red solid was dissolved in DCM and washed with aqueous solutions of ammonium chloride and potassium carbonate. The organic layer was dried on $MgSO_4$ and then filtered. After the solvent was removed under reduced pressure, the crude product was purified by silica gel column chromatography using *n*-hexane/DCM (7:3 v/v) as eluent. A mixture of 1,1′-bis[2-(4-bromophenyl)vinyl]ferrocene isomers with (*Z*,*Z*)-, (*E*,*Z*)-, and (*E*,*E*)-configurations was obtained in 86.8% yield (2.854 g). Recrystallization from hexanes gave the (*E*,*E*)-isomer (**6**), whereas the (*Z*,*Z*)- and (*Z*,*E*)-isomers remained in the solution.

Isomerization of (*Z*,*Z*)- and (*Z*,*E*)-Conformers to an (*E*,*E*)-Conformer. Iodine was added into a mixture of (*Z*,*Z*)- and (*Z*,*E*)-1,1′-bis[2-(4-bromophenyl)vinyl]ferrocenes in hexanes/CH_2Cl_2 (80:20 v/v). The solution was then refluxed for 5 h. After removal of the solvent under reduced pressure, the residue was dissolved in DCM and then treated with an aqueous solution of sodium thiosulfate. The organic layer was dried on $MgSO_4$ and then filtered. Evaporation of the solvent gave pure (*E*,*E*)-1,1′-bis[2-(4-bromophenyl)vinyl] ferrocene (**6**) in a quantitative yield. IR (KBr), ν (cm^{-1}): 1629 (C═C stretching), 1402 (ferrocene), 1006 (ferrocene), 956, 802, 482 (C−Br stretching). ^{1}H NMR (400 MHz, $CDCl_3$), δ (TMS, ppm): 7.31 (d, 4H, J = 6.8 Hz), 7.00 (d, 4H, J = 6.8 Hz), 6.65 (d, 2H, J = 1 4 Hz), 6.32 (d, 2H, J = 14 Hz), 4.61 (s, 4H), 4.43 (s, 4H). Anal. Calcd for $C_{26}H_{20}Br_2Fe$: C, 56.98; H, 3.68. Found: C, 56.80; H, 3.70.

Preparation of (*E*,*E*)-1,1′-Bis(2-{4-[2-(hydroxydimethylmethyl)ethynyl]phenyl}vinyl)ferrocene (8). In a three-necked, round-bottomed flask under argon were placed 1.096 g (2 mmol) of (*E*,*E*)-1,1′-bis[2-(4-bromophenyl)vinyl]ferrocene (**6**), 0.070 g (0.1 mmol) of dichlorobis(triphenylphosphine)palladium(II), 0.052 g (0.2 mmol) of triphenylphosphine, and 0.038 g (0.2 mmol) of copper(I) iodide. Freshly distilled triethylamine (100 mL) and 0.42 mL (5 mmol) of 2-methyl-3-butyn-2-ol (**7**) were then added. The resulting mixture was stirred at 50 °C for 24 h. After solvent evaporation, the solid was dissolved in DCM and washed with aqueous solution of NH_4Cl. The organic layer was dried over $MgSO_4$ and then filtered. The solvent was removed under reduced pressure and the crude product was purified by silica gel column chromatography using *n*-hexane/ethyl acetate (70:30 v/v) as eluent. A mixture of (*E*)-1-(2-{4-[2-(hydroxydimethylmethyl)ethynyl]phenyl}vinyl)-1′-[2-(4-bromophenyl)vinyl]ferrocene and (*E*,*E*)-1,1′-bis(2-{4-[2-(hydroxydimethylmethyl)ethynyl]phenyl}vinyl)ferrocene (**8**) in mole ratio of 3:1 was obtained in 56.3% yield (0.865 g).

Preparation of (*E*,*E*)-1,1′-Bis[2-(4-ethynylphenyl)vinyl]ferrocene (1). In a three-necked, round-bottomed flask under argon was placed 1.109 g (2 mmol) of (*E*,*E*)-1,1′-bis(2-{4-[2-(hydroxyldimethyl−methyl)ethynyl]phenyl}vinyl)ferrocene (**8**) in 0.4 g of NaOH in dry toluene. The mixture was refluxed for 6 h and then filtered. After solvent evaporation, the crude product was purified by silica gel column chromatography using *n*-hexane/DCM (70:30 v/v) as eluent. (*E*,*E*)-1,1′-Bis[2-(4-ethynylphenyl)vinyl]ferrocene (**1**) was obtained in 94.6 yield (0.829 g) as a red solid. IR (KBr), ν (cm^{-1}): 3276 (≡C−H stretching), 2101 (C≡C stretching), 1630 (C═C stretching), 1411 (ferrocene), 1034 (ferrocene), 958, 812, 617. ^{1}H NMR (400 MHz, $CDCl_3$), δ (TMS, ppm): 7.35 (d, 4H, J = 7.6 Hz), 7.18 (d, 4H, J = 7.6 Hz), 6.75 (d, 2H, J = 15.6 Hz), 6.51 (d, 2H, J = 15.6 Hz), 4.50 (s, 4H), 4.34 (s, 4H), 3.14 (s, 2H). ^{13}C NMR (100 MHz, $CDCl_3$), δ (ppm): 138.0, 132.3, 127.4, 125.8, 125.5, 120.1, 84.1, 83.9, 77.5, 70.3, 68.2. TOF−MS (EI): *m*/*z* calcd for $C_{30}H_{22}Fe$ 438.34; found 438 (M^+). Anal. Calcd for $C_{30}H_{22}Fe$: C, 82.20; H, 5.06. Found: C, 81.54; H, 5.42.

Preparation of 1-[2-(4-Bromophenyl)vinyl]ferrocene (10). This compound was prepared by the reaction of 4-bromobenzyltriphenylphosphonium bromide (**4**) with ferrocenecarboxaldehyde (**9**) in the presence of potassium *tert*-butoxide. The experimental procedures were similar to those used for the preparation of the 1,1′-bis[2-(4-bromophenyl)ferrocene isomers. Yield: 93.7%. Recrystallization from hexanes gave the *E*-isomer, whereas the *Z*-isomer remained in the solution.

(*Z*)-to-(*E*) Isomerization. (*Z*)-1-[2-(4-Bromophenyl)vinyl]ferrocene was converted into its *E* isomer by reflux its hexane solution in the presence of iodine. IR (KBr), ν (cm^{-1}): 1632 (C═C stretching), 1403 (ferrocene), 1003 (ferrocene), 961, 806, 483 (C−Br stretching). ^{1}H NMR (400 MHz, $CDCl_3$), δ (TMS, ppm): 7.44 (d, 2H, J = 8 Hz), 7.28 (d, 2H, J = 8 Hz), 6.86 (d, 1H, J = 16 Hz), 6.59 (d, 1H, J = 16 Hz), 4.50 (s, 2H), 4.34 (s, 2H), 4.17 (s, 5H). Anal. Calcd for $C_{18}H_{15}BrFe$: C, 58.90; H, 4.12; Found: C, 59.14; H, 4.17.

Preparation of (*E*)-1-(2-{4-[2-(Hydroxydimethylmethyl)ethynyl]phenyl}vinyl)ferrocene (11). This compound was prepared by the reaction of (*E*)-1-[2-(4-bromophenyl)vinyl]ferrocene (**10**) with 2-methyl-3-butyn-2-ol (**7**), using dichlorobis(triphenylphosphine)palladium(II), triphenylphosphine, and copper(I) iodide as catalysts. The experimental procedures were similar to those used for the preparation of (*E*,*E*)-1,1′-bis(2-{4-[2-(hydroxydimethylmethyl)ethynyl]phenyl}vinyl)ferrocene (**8**). Orange solid was obtained; yield 92.6% (0.686 g).

Preparation of (*E*)-1-[2-(4-Ethynylphenyl)vinyl]ferrocene (2). This monomer was prepared by the base-catalyzed hydrolysis of (*E*)-1-(2-{4-[2-(hydroxydimethylmethyl)ethynyl]phenyl}vinyl)-ferrocene (**11**) in toluene to give a red solid; yield 97.0% (0.606 g). IR (KBr), ν (cm^{-1}): 3264 (≡C−H stretching), 2099 (C≡C stretching), 1632 (C═C stretching), 1691 (ferrocene), 1411 (ferrocene), 1026 (ferrocene), 968, 814, 625. ^{1}H NMR (400 MHz, $CDCl_3$), δ (TMS, ppm): 7.46 (d, 2H, J = 8 Hz), 7.37 (d, 2H, J = 8 Hz), 6.90 (d, 1H, J = 16 Hz), 6.63 (d, 1H, J = 16 Hz), 4.55 (s, 2H), 4.38 (s, 2H), 4.20 (s, 5H), 3.13 (s, 1H). ^{13}C NMR (100 MHz, $CDCl_3$), δ (ppm): 138.4, 132.4, 128.6, 125.6, 125.1, 120.0, 84.0, 82.9, 77.6, 69.3, 69.3, 67.0. TOF−MS (EI): *m*/*z* calcd for $C_{20}H_{16}Fe$ 312.19; found 312 (M^+). Anal. Calcd for $C_{20}H_{16}Fe$: C, 76.95; H, 5.17. Found: C, 76.83; H, 5.26.

Polymer Synthesis. All the copolycyclotrimerization reactions were carried out under nitrogen using standard Schlenk techniques. Given below is a typical experimental procedure for the copolymerization of **1** with **2** under the conditions given in Table 1, no. 2.

Into a thoroughly baked and carefully evacuated 15 mL Schlenk tube with a three-way stopcock on the sidearm were placed 16.1 mg of $TaCl_5$ (0.045 mmol) and 19.2 mg of Ph_4Sn (0.045 mmol) in

a glovebox. Freshly distilled toluene (2.0 mL) was injected into the tube using a hypodermic syringe and the mixture was aged at room temperature for 15 min. A solution of 43.8 mg (0.1 mmol) of **1** and 31.2 mg (0.1 mmol) of **2** in 4.0 mL toluene was then added dropwise into the catalyst solution. After stirring at room temperature for 30 min, the reaction was quenched by the addition of a small amount methanol. The mixture was added dropwise to 300 mL of methanol under vigorous stirring. The precipitate was allowed to stand overnight and then collected by filtration. The crude product was redissolved in THF and dropped into *n*-hexane through a cotton filter under stirring to further purify the copolymer. The product was washed with acetone and dried under vacuum at room temperature to a constant weight. A dark red powdery product was obtained in 95.9%. IR (KBr), ν (cm^{-1}): 1630 (C═C stretching), 3083, 1105 (ferrocene), 954, 810. ^{1}H NMR (400 MHz, $CDCl_3$), δ (TMS, ppm): 6.68−7.62 (Ar−H), 6.13−6.68 (CH═CH), 4.31−4.50 (Cp−H_4), 4.16 (Cp−H_5).

Cobalt Complexation. Into a 30 mL test tube was dissolved 42.1 mg of an *hp*-PFP (sample from Table 1, no. 9) in 10 mL of THF under nitrogen. A THF solution of $Co_2(CO)_8$ (5 mL, 60 mg) was added. The solution was stirred at room temperature for 1 h, after which the solvent was evaporated to about half of its original volume under reduced pressure. The solution was then added dropwise into a large amount of hexanes (∼200 mL) under stirring. The precipitate was washed with hexanes several times to remove unreacted octacarbonyldicobalt and dried under vacuum to a constant weight. A brown powder was obtained.

Pyrolytic Ceramization. Ceramics were prepared from *hb*-PFPs and their cobalt complexes by the pyrolyses in a Lindberg/Blue tube furnace with a heating capacity up to 1700 °C. In a typical run, 53.5 mg of an *hb*-PFP (sample from Table 1, no. 8) was placed in a porcelain crucible, which was heated to 1000 °C at a heating rate of 10 °C/min in a nitrogen stream at a flow rate of 0.2 L/min. The sample was sintered for 1 h at 1000 °C. A black ceramic was obtained in 52.9% yield (28.3 mg) after cooling to room temperature.

Acknowledgment. This work was partially supported by the National Natural Science Foundation of China (20474007 and 20634020) and the Research Grants Council of Hong Kong (604903).

References and Notes

(1) (a) Wong, W. Y.; Liu, L.; Poon, S. Y.; Choi, K. H.; Cheah, K. W.; Shi, J. X. *Macromolecules* **2004**, *37*, 4496−4504. (b) Lam, J. W. Y.; Luo, J.; Dong, Y.; Cheuk, K. K. L.; Tang, B. Z. *Macromolecules* **2002**, *35*, 8288−8299. (c) MacLachlan, M. J.; Ginzburg, M.; Coombs, N.; Raju, N. P.; Greedan, J. E.; Ozin, G. A.; Manners, I. *J. Am. Chem. Soc.* **2000**, *122*, 3878−3891. (d) Hinderling, C.; Keles, Y.; Stöckli, T.; Knapp, H. F.; de los Arcos, T.; Oelhafen, P.; Korczagin, I.; Hempenius, M. A.; Vancso, G. J.; Pugin, R.; Heinzelmann, H. *Adv. Mater.* **2004**, *16*, 876−879. (e) Gregson, C. K. A.; Gibson, V. C.; Long, N. J.; Marshall, E. L.; Oxford, P. J.; White, A. J. P. *J. Am. Chem. Soc.* **2006**, *128*, 7410−7411. (f) D'Souza, F.; Chitta, R.; Gadde, S.; Shafiqul Islam, D.-M.; Schumacher, A. L.; Zandler, M. E.; Araki, Y.; Ito, O. *J. Phys. Chem. B* **2006**, *110*, 25240−25250.

(2) (a) Lu, J. Q.; Kopley, T. E.; Moll, N.; Roitman, D.; Chamberlin, D.; Fu, Q.; Liu, J.; Russell, T. P.; Rider, D. A.; Manners, I.; Winnik, M. A. *Chem. Mater.* **2005**, *17*, 2227−2231. (b) Caruana, D. J.; Heller, A. *J. Am. Chem. Soc.* **1999**, *121*, 769−774.

(3) (a) Wu, S.; Chen, Y.; Zeng, F.; Gong, S.; Tong, Z. *Macromolecules* **2006**, *39*, 6796−6799. (b) Ferreira, C. L.; Ewart, C. B.; Barta, C. A.; Little, S.; Yardley, V.; Martins, C.; Polishchuk, E.; Smith, P. J.; Moss, J. R.; Merkel, M.; Adam, M. J.; Orvig, C. *Inorg. Chem.* **2006**, *45*, 8414−8422. (c) Dardel, B.; Deschenaux, R.; Even, M.; Serrano, E. *Macromolecules* **1999**, *32*, 5193−5198. (d) Nlate, S.; Ruiz, J.; Astruc, D.; Blais, J. C. *Chem. Commun.* **2000**, 417−418. (e) Cardona, C. M.; McCarley, T. D.; Kaifer, A. E. *J. Org. Chem.* **2000**, *65*, 1857−1864. (f) Turrin, C. O.; Chiffre, J.; Daran, J. C.; de Montauzon, D.; Caminade, A. M.; Manoury, E.; Balavoine, G.; Majoral, J. P. *Tetrahedron* **2001**, *57*, 2521−2536. (g) Even, M.; Heinrich, B.; Guillon, D.; Guldi, D. M.; Prato, M.; Deschenaux, R. *Chem.−Eur. J.* **2001**, *7*, 2595−2604. (h) Kim, C.; Park, E.; Song, C. K.; Koo, B. W. *Synth. Met.* **2001**, *123*, 493−496. (i) Ashton, P. R.; Balzani, V.; Clemente-Leon, M.; Colonna, B.; Credi, A.; Jayaraman, N.; Raymo, F. M.; Stoddart, J. F.; Venturi, M. *Chem.−Eur. J.* **2002**, *8*, 673−684. (j) Bernard, J.; Schappacher, M.; Ammannati, E.; Kuhn, A.; Deffieux, A. *Macromolecules* **2002**, *35*, 8994−9000. (k) Sengupta, S. *Tetrahedron Lett.* **2003**, *44*, 7281−7284.

(4) (a) Abd-Elzaher, M. M.; Hegazy, W. H.; Gaafar, A. E. *Appl. Organomet. Chem.* **2005**, *19*, 911−916. (b) *Frontiers in Transition Metal-Containing Polymers*; Abd-El-Aziz, A. S., Manners, I., Eds.; Wiley: Hoboken, NJ, 2007. (c) *Macromolecules Containing Metal and Metal-Like Elements, Transition Metal-Containing Polymers*; Abd-El-Aziz, A. S., Jr., Carraher, C. E., Jr., Pittman, C. U., Sheats, J. E., Zeldin, M., Eds.; Wiley: Hoboken, NJ, 2004.

(5) (a) Foucher, D. A.; Tang, B. Z.; Manners, I. *J. Am. Chem. Soc.* **1992**, *114*, 6246−6248. (b) Fossum, E.; Matyjaszewski, K.; Rulkens, R.; Manners, I. *Macromolecules* **1995**, *28*, 401−402. (c) Manners, I. *J. Polym. Sci., Part A: Polym. Chem.* **2002**, *40*, 179−191. (d) Petersen, R.; Foucher, D. A.; Tang, B. Z.; Lough, A.; Raju, N.; Greedan, J.; Manners, I. *Chem. Mater.* **1995**, *7*, 2045−2053. (e) Foucher, D. A.; Ziembinski, R.; Tang, B. Z.; McDonald, P.; Massey, J.; Raimund, J.; Vancso, J.; Manners, I. *Macromolecules* **1993**, *26*, 2878−2884.

(6) (a) Kloninger, C.; Rehahn, M. *Macromolecules* **2004**, *37*, 1720−1727. (b) Temple, K.; Kulbaba, K.; Power-Billard, K. N.; Manners, I.; Leach, K. A.; Xu, T.; Russell, T. P.; Hawker, C. J. *Adv. Mater.* **2003**, *15*, 297−300. (c) Eitouni, H. B.; Balsara, N. P. *J. Am. Chem. Soc.* **2004**, *126*, 7446−7447. (d) Kim, K. T.; Han, J.; Ryu, C. Y.; Sun, F. C.; Sheiko, S. S.; Winnik, M. A.; Manners, I. *Macromolecules* **2006**, *39*, 7922−7930. (d) Foucher, D. A.; Honeyman, C. H.; Nelson, J. M.; Tang, B. Z.; Manners, I. *Angew. Chem., Int. Ed.* **1993**, *32*, 1709−1711. (e) Tang, B. Z.; Petersen, R.; Foucher, D. A.; Lough, A.; Coombs, N.; Sodhi, R.; Manners, I. *J. Chem. Soc., Chem. Commun.* **1993**, 523−525.

(7) (a) Abd-El-Aziz, A. S.; Todd, E. K.; Afifi, T. H. *Macromol. Rapid Commun.* **2002**, *23*, 113−117. (b) Abd-El-Aziz, A. S.; Afifi, T. H.; Budakowski, W. R.; Friesen, K. J.; Todd, E. K. *Macromolecules* **2002**, *35*, 8929−8932.

(8) Sun, Q.; Xu, K.; Peng, H.; Zheng, R.; Haussler, M.; Tang, B. Z. *Macromolecules*, **2003**, *36*, 2309−2320.

(9) For reviews, see: (a) Häussler, M.; Qin, A.; Tang, B. Z. *Polymer* **2007**, *48*, in press. (b) Häussler, M.; Tang, B. Z. *Adv. Polym. Sci.* **2007**, *209*, 1−58. (c) Häussler, M.; Dong, H. C.; Lam, J. W. Y.; Zheng, R.; Qin, A.; Tang, B. Z. *Chinese J. Polym. Sci.* **2005**, *23*, 567−591. (d) Dong, H.; Lam, J. W. Y.; Häussler, M.; Zheng, R.; Peng, H.; Law, C. C. W.; Tang, B. Z. *Curr. Trends Polym. Sci.* **2004**, *9*, 15−31. (e) Häussler, M.; Lam, J. W. L.; Zheng, R.; Peng, H.; Luo, J. D.; Chen, J. W.; Law, C. C.; Tang, B. Z. *C. R. Chim.* **2003**, *6*, 833−842.

(10) (a) Zheng, R.; Dong, H.; Peng, H.; Lam, J. W. Y.; Tang, B. Z. *Macromolecules* **2004**, *37*, 5196−5210. (b) Dong, H.; Zheng, R.; Lam, J. W. Y.; Häussler, M.; Qin, A.; Tang, B. Z. *Macromolecules* **2005**, *38*, 6382−6391.

(11) (a) Chen, J.; Peng, H.; Law, C. C. W.; Dong, Y.; Lam, J. W. Y.; Williams, I. D.; Tang, B. Z. *Macromolecules* **2003**, *36*, 4319−4327. (b) Xu, K.; Peng, H.; Sun, Q.; Dong, Y.; Salhi, F.; Luo, J.; Chen, J.; Huang, Y.; Zhang, D.; Xu, Z.; Tang, B. Z. *Macromolecules* **2002**, *35*, 5821−5834. (c) Peng, H.; Cheng, L.; Luo, J.; Xu, K.; Sun, Q.; Dong, Y.; Salhi, F.; Lee, P. P. S.; Chen, J.; Tang, B. Z. *Macromolecules* **2002**, *35*, 5349−5351. (d) Xu, K.; Tang, B. Z. *Chin. J. Polym. Sci.* **1999**, *17*, 397−402. (e) Peng, H.; Luo, J.; Cheng, L.; Lam, J. W. Y.; Xu, K.; Dong, Y.; Zhang, D.; Huang, Y.; Xu, Z.; Tang, B. Z. *Opt. Mater.* **2002**, *21*, 315−320. (f) Li, Z.; Qin, A.; Lam, J. W. Y.; Dong, Y.; Dong, Y.; Ye, C.; Williams, I. D.; Tang, B. Z. *Macromolecules* **2006**, 39, 1436−1442.

(12) Li, Z.; Lam, J. W. Y.; Dong, Y.; Dong, Y.; Sung, H. H. Y.; Williams, I. D.; Tang, B. Z. *Macromolecules* **2006**, *39*, 6458−6466.

(13) Shi, J.; Tong, B.; Zhao, W.; Shen, J.; Zhi, J.; Dong, Y.; Häussler, M.; Lam, J. W. Y.; Tang. B. Z. *Macromolecules* **2007**, *40*, 5612−5617.

(14) (a) Liu, K.; Clendenning, S. B.; Friebe, L.; Chan, W. Y.; Zhu, X.; Freeman, M. R.; Yang, G. C.; Yip, C. M.; Grozea, D.; Lu, Z. H.; Manners, I. *Chem. Mater.* **2006**, *18*, 2591−2601. (b) Häussler, M.; Zheng, R.; Lam, J. W. Y.; Tong, H.; Dong, H.; Tang, B. Z. *J. Phys. Chem. B.* **2004**, *108*, 10645−10650.

(15) (a) Rodríguez, J. G.; Gayo, G.; Fonseca, I. *J. Organomet. Chem.* **1997**, *534*, 35−42. (b) Rodríguez, J. G.; Pleite, S. *J. Organomet. Chem.* **2001**, *637*, 230−239.

(16) Xu, K.; Peng, H.; Sun, Q.; Dong, Y.; Salhi, F.; Luo, J.; Chen, J.; Huang, Y.; Zhang, D.; Xu, Z.; Tang, B. Z. *Macromolecules* **2002**, *35*, 5821−5834.

(17) (a) Grayson, S. M.; Frechet, J. M. J. *Macromolecules* **2001**, *34*, 6542−6544. (b) Muchtar, Z.; Schappacher, M.; Deffieux, A. *Macromolecules* **2001**, *34*, 7595−7600. (c) Peng, H.; Lam, J. W. Y.; Tang, B. Z. *Polymer* **2005**, *46*, 5746−5751. (d) Bosman, A. W.; Janssen, H. M.; Meijer, E. W. *Chem. Rev.* **1999**, *99*, 1665−1688. (e) Murayama, M.;

Okada, M.; Fukutomi, T.; Nose, T. *Macromol. Chem. Phys.* **1987**, *188*, 829−843.
(18) Heilmann, J. B.; Scheibitz, M.; Qin, Y.; Sundararaman, A.; Jakle, F.; Kretz, T.; Bolte, M.; Lerner, H. W.; Holthausen, M. C.; Wagner, M. *Angew. Chem., Int. Ed.* **2006**, *45*, 920−925.
(19) (a) Jayakumar, N. K.; Bharathi, P.; Thayumanavan, S. *Org. Lett.* **2004**, *6*, 2547−2550. (b) Cardona, C. M.; Kaifer, A. E. *J. Am. Chem. Soc.* **1998**, *120*, 4023−4024. (c) Stone, D. L.; Smith, D. K.; McGrail, P. T. *J. Am. Chem. Soc.* **2002**, *124*, 856−864. (d) Labande, A.; Ruiz, J.; Astruc, D. *J. Am. Chem. Soc.* **2002**, *124*, 1782−1789. (e) Cardona, C. M.; McCarley, T. D.; Kaifer, A. E. *J. Org. Chem.* **2000**, *65*, 1857−1864.
(20) Matas, J.; Uriel, S.; Peris, U.; Llusar, R.; Houbrechts, S.; Persoons, J. *J. Organomet. Chem.* **1998**, *562*, 197−202.
(21) (a) *Dictionary of Organometallic Compounds*; Buckingham, J., Ed.; Chapman and Hall: London, 1984. (b) Elschenbroich, C.; Salzer, A. *Organometallics*, 2nd ed.; VCH: Weinheim, Germany, 1992.
(22) Sun, Q.; Lam, J. W. Y.; Xu, K.; Xu, H.; Cha, J. A. P.; Wong, P. C. L.; Wen, G.; Zhang, X.; Jing, X.; Wang, F.; Tang, B. Z. *Chem. Mater.* **2000**, *12*, 2617−2624.
(23) Tang, B. Z.; Geng, Y.; Lam, J. W. Y.; Li, B.; Jing, X.; Wang, X.; Wang, F.; Pakhomov, A. B.; Zhang, X. X. *Chem. Mater.* **1999**, *11*, 1581−1589.
(24) Berenbaum, A.; Ginzburg-Margau, M.; Coombs, N.; Lough, A. J.; Safa-Sefat, A.; Greedan, J. E.; Ozin, G. A.; Manners, I. *Adv. Mater.* **2003**, *15*, 51−55.

MA071019Q